Indonesian Journal of Electrical Engineering and Informatics (IJEEI)
Vol. 13, No. 1, March 2025, pp. 169~183
ISSN: 2089-3272, DOI: 10.52549/ijeei.v13i1.6170

Methodological Approach to Automated Recognition of Atrial Fibrillation and Subsequent Classification

Abas Lampezhev[1], Naur Ivanov[2], Tagirbek Aslanov[3], Muhamed Nogmov[4], Viktor Lysenko[5]
[1,2,3,4,5]Institute of Design and Technology Informatics, Russian Academy of Sciences, Moscow, Russia

Article Info

Article history:

Received Dec 26, 2024
Revised Mar 6, 2025
Accepted Mar 13, 2025

Keywords:

Heart rhythm disorders
Atrial fibrillation (AF)
Cardiological diagnostics
K-entropy
Nonlinear dynamics

ABSTRACT

This study considers topical issues aimed at improving the methodology of early recognition of atrial fibrillation and monitoring its treatment against the background of other heart rhythm disorders. The task set in this study is an essential component of the search for solutions, whose purpose is to increase the efficiency of information systems for cardiac diagnostics and monitoring within the framework of complex research to improve the means of heart rhythm analysis and arrhythmia recognition. In the context of this study, a linear discriminant analysis approach based on the concept of K-entropy was proposed as a means of automating the procedure for the recognition of AF against the background of other rhythm disorders using a limited data sample. With regard to the classification of atrial fibrillation samples, the use of decisive rules and arrhythmia types, based on the analysis of scatterograms, is put forth as a solution. The results of the proposed methods for recognizing the presence of atrial fibrillation and its classification demonstrated superior performance when compared to existing methods. The proposed method exhibited a specificity of 98.5% and a sensitivity of 98%. The proposed method for determining the presence of atrial fibrillation demonstrates suboptimal accuracy when applied to a limited sample size. Further development of the method should be concentrated in this area.

Corresponding Author:

Abas Lampezhev,
Institute of Design and Technology Informatics,
Russian Academy of Sciences,
18 Vadkovsky Lane, building 1a, Moscow, 127055, Russian Federation.
Email: abas.lampezhev@mail.ru

1. INTRODUCTION

Therapy that uses the results of biomedical research assists in forming the latest variations in the electronic processing of specific information and improving the methods of reliable identification of biological impulses [1]. Modern medical information systems can accurately determine a patient's current state and assess the heart rate variability (HRV), reflecting, in general, the specificity of physiological functions. Such noninvasive studies aimed at risk stratification and diagnostics are especially relevant for patients with diseases of the cardiovascular system (CVS), whose condition reflects the work of almost all body systems [2, 3].

The main task of automating ECG analysis in cardiac detection, monitoring, and diagnostic systems is to ensure reliable recognition of dangerous arrhythmias at the moment of their first signs. Most existing methods that solve this problem rely on spectral analysis of electrical cardiac impulses, which are limited to an inefficient list of classifying characteristics. Optimization of the decisive rule (their set), which guarantees the detection of pathological rhythms, is critical for the modernization of electronic complexes that offer continuous monitoring of a patient's current state [4, 5].

Currently, the critical issue related to the automation of research activities in cardiology is the identification of arrhythmias characterized by chaotic changes in the cardiac cycle duration, which is confirmed by the statistical fact that in more than 80% of patients, the recorded chain of cardiac cycles is spontaneous.

The main difficulty in creating automated atrial fibrillation (AF) diagnosis methods is the lack of effective mathematical models that clearly describe the nature of heartbeat disorders.

Currently, one of the most significant challenges in the automation of cardiological studies that necessitates practical solutions is the identification of arrhythmias, which are characterized by random (chaotic) alterations in cardiac cycle duration (AF).

The number of patients with atrial fibrillation (AF) has dramatically increased in recent years. The transition to automation of cardiac monitoring in patients with AF will help solve a number of problems, including the prevention of thromboembolic episodes, which are extremely life-threatening for patients, the evaluation of electrophysiological risk factors in the process of development of this disorder, the optimization of medical treatment tactics, and the decision on the use of artificial cardiac pacing. The advancement of theory and analytical techniques for identifying irregularities in cardiac rhythm, particularly those exhibiting chaotic behavior in their interval sequences, provides a foundation for addressing these challenges.

In addition, in arrhythmia recognition systems, it is important to consider the interference arising during ECG signal processing. The solution to this problem is provided by the significant computational resources of modern technical means, which allow us to move to more complex and efficient preprocessing procedures.

The aim of this study was to improve tools for heart rhythm analysis, arrhythmia recognition, and classification. Among a wide range of tasks contributing to the goal, this study is devoted to the development of a methodological approach to automate early AF recognition based on the description of chaotic processes, as well as the definition of decisive rules for detection and classification.

2. FEATURES OF THE EXISTING METHODOLOGICAL APPROACHES PROVIDING ARRHYTHMIA RECOGNITION

Today, many different quantitative and visual methodological approaches aim to analyze heart rhythms and recognize arrhythmias based on the study of various indicators that reflect their nature from temporal (within statistical and geometric approaches) and frequency perspectives.

Arrhythmias are diagnosed according to their classification based on the methods of analysis and the degree of danger of cardiac pathologies for the patient. Atrial fibrillation is characterized by irregular changes in the duration of RR-intervals and the presence of atrial fibrillation waves, which are recognized in the mode of continuous ECG monitoring, usually by using graphical methods of rhythm analysis, including the construction of a scatterogram and analysis of the histogram of RR-intervals. These disorders are recognized by the absence of R-beats at the output of the ventricular complex detector when analyzing short ECS fragments (several seconds) or in cases of unstable detection [6, 7].

Some approaches rely on the study of rhythmograms (visual and logical investigations of wave structures of heart rhythms), spectral estimation, rhizomorphic estimation, the use of nonlinear dynamics (based on the theoretical foundations of deterministic chaoses), and variation pulsometry (estimation of characteristics of univariate and multivariate sequences, and determination of the secondary indicator of univariate distributions) [8].

The primary purpose of temporal analysis of HRV within a specific time domain is to assess the severity of existing sinus arrhythmia. The basis for statistical methods is to determine the duration of consecutive intervals and the exact dimensions for the sequence of normal cardiac intervals.

As artificial intelligence (AI) continues to transform the practice of medicine, this review article identifies and examines specific applications of AI in the screening, diagnosis, and treatment of AF. The incorporation of AI algorithms has markedly enhanced the capabilities of routine digital devices and diagnostic technology, thereby expanding the scope of large-scale population-based screening and diagnostic assessments. Similarly, these technologies have affected the treatment pathway of AF, facilitating the identification of patients who may benefit from specific therapeutic interventions. Although the application of AI to the diagnostic and therapeutic pathways of AF has been remarkably successful, it is imperative to consider the potential shortcomings and constraints of these algorithms [9].

The essence of geometric methods is the construction of a density function for the distribution of specific histograms with subsequent analysis of the shape parameters. It is essential to consider that many mathematical models can be used to describe the geometric image of such a histogram, such as linear or triangular. Subsequently, a mandatory analysis of the parameters obtained for the developed mathematical model is performed. Triangular interpolation is the most widely used method [10].

As practical experience shows, all heart rhythm changes have a quasiperiodic character, making them extremely difficult to detect within a specific time domain. Various spectral analysis approaches have been used to study these properties.

The results of many studies emphasize the prospect of using the mechanism of heart rhythm regulation and various methodological approaches to nonlinear dynamics, in which the definition of a specific phase portrait, construction of spatial maps, and calculation of dimensionality and entropy play a particular role.

The support vector machine is also a popular method for detecting AF. The detection method used the RR interval variability or HRV. Variability is an essential characteristic of atrial fibrillation in which the heart may beat with an irregular rhythm opposite to the regular rhythm characteristic of a normal heart. Thus, electrocardiographic rhythms are essential for the detection of AF. The findings of numerous studies have yielded several significant implications regarding the use of the SVM method for AF detection of atrial fibrillation. SVM invariants represent a robust technique for differentiating various cardiac arrhythmias. They effectively capture pertinent information from electrocardiogram (ECG) signals, thereby facilitating accurate classification into multiple categories. Although linear SVM demonstrated the most optimal performance, kernelized SVM exhibited superior outcomes owing to its capacity to capture random patterns, underscoring the necessity of selecting appropriate algorithms for the classification of arrhythmia activity [11].

Variations in electrocardiographic features for arrhythmia detection are essential for a good performance. Therefore, a variation of the two features is proposed, which can provide the best performance of 95.81% and 98.44% in terms of sensitivity and specificity, respectively [12].

Today, medicine offers several functional techniques for automated AF diagnostics, such as techniques based on wavelet transforms of ECG impulses, studies of abnormalities using other ECG diagnostic formats, and techniques related to processing separated ECG impulses. Thus, the principle of the separate transformation of extreme impulses obtained after excluding all QRS complexes from the working ECG was used in this study. The authors obtained many experimental characteristics to identify the waves transmitting atrial flutter. Currently, the algorithm of automated AF diagnostics demonstrates a sufficiently low performance of 62.92%, but the modernization of this approach continues [13, 14].

To improve the efficiency of AF detection, some principles of contextual analysis of complex impulses obtained by double differentiation of residual ECG can be used as an auxiliary tool. Using the two-stage complex computational search procedure proposed by the authors, the detection of false waves was minimized. According to the results of experimental analysis, the AF detection rate exceeded 80% [15].

To quantitatively evaluate atrial function, we studied differentiated ECGs that had undergone several low-pass filtering cascades. The results obtained from a limited number of experiments showed that the known characteristics of *f*-wave morphology can provide more efficient AF detection rates of 89% [16].

The abovementioned methods of detailed analysis of characteristic features of *f*-waves of ECG cannot provide reliable detection of the atrial wave spectrum under the constant influence of background noise and do not meet the majority of modern requirements for real-time work. Specialized professionals still have no tools for the timely detection of these disorders.

Practical AF detection tasks often use graphical techniques to perform rhythm analysis, based on the study of constructed scatterograms, histograms of any temporal impulse, and 3D scatterograms.

Notably, the efficiency of these techniques in the analysis of beat variability is sufficiently high. Interval histograms are a popular tool for assessing the level of typical arrhythmias expressed by their transition from monomodal to multimodal forms. This study showed that modern correlative rhythmography allows us to classify the five main variants of these dependence curves. It opens broad prospects in standard clinical conditions to perform professional assessment of atrioventricular nodes to predict cardiac muscle response to various forms of influence, among others. This study shows that investigations of multidimensional scatterograms can become the basis for rhythmogram composition observations.

Today, these techniques offer visual formats for informing the patient's cardiac muscle functioning, that is, they represent visual techniques for studying chains of cardiac cycles. Simultaneously, some results are intermediate, as they relate to the standard sinus beat, which makes the diagnosis of these diseases easier.

The study of training artificial neural networks using preliminary wavelet transforms of heartbeat characteristics is also attractive. The authors noted that the analysis demonstrated good possibilities for using this technique in considering rhythmograms, and it is sufficiently promising [17].

The first technique for arrhythmia detection is to create a cascade of filters to predict future errors, which indicates a random change in the studied order of cardiac periods. The second technique enables the estimation of the conditional entropy. The study of changes in the characteristics under consideration over time (we are discussing the increase in the chain length of the signs representing the considered phenomenon) is often a highly effective tool that measures the irregularity of the operation of the systems generating this chain with sufficiently high accuracy. The third technique uses deterministic chaos, which allows for an approximate estimation of the K-entropy to analyze chaotic momentum variation by operating with limited sets [18, 19].

Well-known techniques can be used to detect complications of AF. They used cardiac cycle chains to analyze autoregression spectra with high accuracy and estimated the conditional entropies. The principles of using a new approach in electrocardiographic studies rest on the integrated analysis of a complex system characterized by nonlinear dynamics.

The considered approach that allows for the guaranteed detection of AF can be reduced to the format of a mathematical model that acts according to the behavior of random processes as follows:

- Discrete-time series with weakly correlated counts;
- Irregular time series;
- Complex processes with a clear chaotic component.

Automated methods for the classification of atrial fibrillation (AF) episodes typically depend on the analysis of electrocardiogram (ECG) signals. The absence of intermittent P waves or the presence of fibrillatory F waves on the ECG (seen as wave-like fluctuations of the isoelectric baseline), in conjunction with irregular heart rate fluctuations, are hallmarks of AF. Despite considerable progress in understanding the factors contributing to atrial fibrillation episodes, the development of automated methods to detect AF episodes is still far from achieving satisfactory results because of several contributing factors, such as the presence of external noise, especially due to electrode and patient motion, which severely degrades the performance of AF classifiers, leading to an increase in classification errors, which becomes even more important in the context of modern wearable sensors. The use of wearable sensors for ECG recording and subsequent monitoring of arrhythmias has garnered significant interest [20]. Contemporary wearable sensors provide cost-effective and convenient solutions for vital function monitoring; nevertheless, they exhibit considerable susceptibility to noise interference and are highly sensitive to motion artifacts. This necessitates the development of an AF classifier that is robust to noise while being able to accurately identifying AF rhythms, particularly in the presence of other similar arrhythmias [21].

The model described by the regularities of nonlinear dynamic system behavior (attractor dimension, Lyapunov exponent, and Kolmogorov entropy) makes it possible to obtain the base characteristics for this process and analyze the parameters of biological impulses, reflecting, for example, pathological deviations in the order of heart rhythms.

3. MODEL OF A METHODOLOGICAL APPROACH TO AUTOMATE THE PROCEDURE OF EARLY AF RECOGNI-TION AGAINST THE BACKGROUND OF OTHER RHYTHM DISORDERS USING A LIMITED DATA SAMPLE

The mathematical apparatus of nonlinear dynamic methods based on the bifurcation theory of dynamic (deterministic) chaos can adequately describe a model that significantly expands the range of criteria for analyzing and diagnosing cardiovascular system states. The advantage of this approach is the possibility of modeling structures and phenomena that are not fully ordered, where it is possible to identify particular algorithms and some predeterminations and describe the chaotic process against the background of seeming disorder. On the other hand, unfortunately, it is not always possible to predict their long-term behavior.

3.1. Definition of the algorithm for finding the approximated entropy

K-entropy (an average indicator of the data loss rate on the current states of the systems under consideration for a particular time) is the main parameter reflecting the specificity of chaotic motion. This parameter describes a system that uses an attractor. In general, this is a subspace of boundaries in which each chaotic trajectory moves. The system can also be characterized by a list of auxiliary data, which makes it possible to predict the cells i^*_{n+1}, and it is possible to find the system when it is certain that the trajectory $i^*_1, i^*_2, \dots, i^*_n$ describes its motion. Suppose that *d*-dimensional spaces consist of cells with dimension l^d, system $X(t)$ can be defined in time intervals τ. In such a case, we represent the *K*-entropy, which allows us to measure chaos using the relation:

$$K = \lim_{\tau\to 0}\lim_{l\to 0}\lim_{N\to\infty} \frac{1}{N\tau}\sum_{n=0}^{N-1}(K_{n+1} - K_n) = -\lim_{\tau\to 0}\lim_{l\to 0}\lim_{N\to\infty} \frac{1}{N\tau}\sum_{i_0 \dots i_N} P_{i_0\dots i_N} \ln P_{i_0\dots i_N} \quad (1)$$

here, $K = -\sum_{i_0\dots i_N} P_{i_0\dots i_N} \ln P_{i_0\dots i_N}$ is the value that is proportional to the data that make it possible to determine the location of systems $i_0 \dots i_N$, and the accuracy of prediction is expressed by the current *l;* $P_{i_0\dots i_N}$ is the value of the joint probability that the system $X(t)$ will stay: concerning $X(t = 0)$ – in cells i_0; concerning $X(t = \tau)$ – in cells i_1;…; concerning $X(t + n\tau)$ – in cells i_n; *N* is the maximum number of analyzed positions of the system.

The limits $l\to 0$ and $N\to\infty$ emphasize the independence of the indicator describing chaos (possibility of chaotic change) from the *K* value. In general, regarding regular motion, *K*-entropy can be equal to zero, and regarding infinite motion, *K*-entropy can be compared with random processes. If the process is constant, it is comparable to the given chaoticity.

Considering impulse behavior, which, at first sight, is sufficiently random, allows us to reveal the information contained in this impulse about the center of attraction. In other words, it is possible to determine the differences between the irregularity characteristic of the motion to the center of attraction and the influence of the noise component on the process under consideration, for which *K*-entropy is used. The calculation of this characteristic is complicated by the presence of only one known component of the studied complex phenomenon. However, the attractors representing the process characteristics are in *d*-dimensional space [22, 23].

Considering Takenson's theorem, we can determine some properties of the point of attraction by analyzing the time sequence of the change in one component describing the process under study [24].

For this purpose, it is essential to determine the *K*-entropy at the lower bound:

$$K_2 = \lim_{\tau \to 0} \lim_{n \to \infty} \frac{1}{n} ln \frac{C_n(l)}{C_{n+1}(l)} \leq K \tag{2}$$

Here, $C_n(l)$ is an integral whose value can be calculated with respect to the orders of the points of infinite length.

In this case, chaos exists when $K_2 > 0$. Simultaneously, the $N \to \infty$ condition does not allow this indicator to be used for finite sets of cardiac impulses.

The analysis of the order of counts of some length *N* implies the need to approximate *K*-entropy. Let us assume that a set of lengths N is characterized by initial data $x(1), x(2),..., x(N)$, and is given by the length of the studied sequence (m) and a threshold limiting the dimensionality of each cell (r), in parallel describing a cascade of filters to separate the noise component. The approximated entropy can be determined using the following algorithm:

1) Sequences $X(1),...,X(N\text{-}m\text{+}2)$ are formed by the relation $X(i) = [x(i), x(i+1), \dots, x(i+m-1)]$, where $i = 1,..., (N\text{-}m\text{+}1)$;

2) The distance between $X(i)$ and $X(j)$ is determined:

$$d[X(i), X(j)] = \max_{k=0,\dots,(m-1)} [|x(i+k) - x(j+k)|] \tag{3}$$

3) The following expression is calculated:

$$C_r^m(i) = \frac{N^m(i)}{(N-m+1)} \tag{4}$$

here, $N^m(i)$ is the number of values $d[X(i), X(j)]$, which satisfy the condition $d[X(i), X(j)] \leq r (j = 1, \dots, (N-m+1))$

4) Natural logarithms for each $C_r^m(i)$ and their average value are calculated

5)

$$\theta^m(r) = \frac{1}{N-m+1} \sum_{i=1}^{N-m+1} ln\, C_r^m\,(i) \tag{5}$$

6) The above-mentioned steps of the procedure for finding the approximated entropy are sequentially repeated for the analyzed data chain of length m+1, that is, $C_r^{m+1}(i)$ and $\theta^{m+1}(r)$ are determined. Therefore, we can approximately estimate the *K*-entropy $ApEn(m,r) = \lim_{N \to \infty} |\theta^m(r) - \theta^m(r)|$, expressed as a limited set by the ratio

$$ApEn(m,r,N) = |\theta^m(r) - \theta^{m+1}(r)| \tag{6}$$

The approximated entropy, which is the dependence of the dimensionality of the studied order *t* on the entire length of the set *N*, is characterized by the fact that, as *m* increases, the value of *ApEn*(*m*) becomes approximately zero, regardless of how regular the process is considered. This is because as *m* increases, the chances that the order data will describe only once-occurring events will naturally increase. Researchers often deal with erroneous values that describe the randomness of the impulse under study when using approximated entropy calculated using this algorithm. To exclude this, the lower value of the corrected estimate describes the *K*-entropy:

$$ApEn_{cor}(m) = ApEn(m) + ApEn(0) \cdot \frac{N_m^{(1)}}{N_{m+1}} \tag{7}$$

in this case, N_{m+1} expresses all considered orders of impulses of length (m +1), $N_m^{(1)}$ is the number of all once emerged orders of length m, $ApEn(0)$ is the absolute entropy calculated for the initial order of counts.

3.2. Determination of atrial fibrillation identification parameters

Figure 1 shows some examples of $ApEn_{cor}(m)$ and $ApEn(m)$ functions from order lengths m determined by models describing a harmonic impulse $s(i)=3cos(\pi i/20)$, $i=1,2,3,....,N$ (a), noise component of 0.09 (b), and a combination of harmonic impulse and noise components (c). Figure 1 (d) shows the function of the number of once-detected orders from m concerning harmonic impulse (1), noise component (2), and their combination (3).

The introduction of the $ApEn_{cor}(m)$ correction and the joint consideration of some characteristic features of the dependencies presented in Figure 1 make it possible to facilitate the solution of the problem of recognizing processes that differ in their regularity. The graphs show that the values of $ApEn(1)$, $ApEn(2)$ and also $ApEn(3)$ concerning the harmonic impulse are smaller than the values describing the noise component and the combination of the noise component with harmonic impulses. In addition, when the harmonic impulses $ApEn(m)$ and $ApEn_{cor}(m)$ are equal when applied to a noisy impulse, they will be significantly different. This phenomenon occurs because the correction is performed considering once identified orders, but considering Figure 1 (d) regarding the harmonic impulse, the value $N_m^{(1)}$ will be zero. However, regarding the noise component and the combination of the helpful impulse with the noise component, the number of these orders increased with increasing m.

Note that the calculation of $ApEn(m,r,N)$ relies on the flexible option of creating each significant region owing to the structure of the hyperspheres shown in Figure 2, having a half-diameter r whose center is given by the values $r = (015)\ 0,27SD_x$, and $m =(1)\ 2, ..., 7(6)$, when SD_x is the error of the initial set.

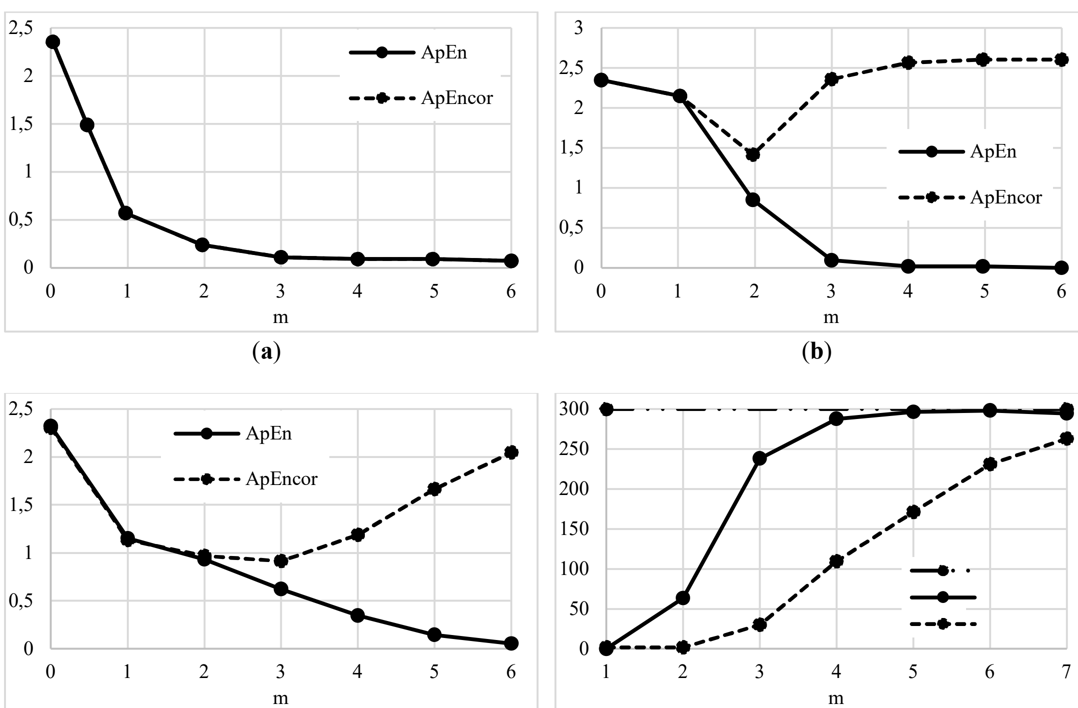

Figure 1. Demonstration examples of ApEn(m) and $ApEn_{cor}(m)$ dependence on the length of chains m, obtained using the following models: a) harmonic impulse, b) noise, c) combination of impulse and noise, d) dependences of the number $N_m^{(1)}$ of single chains

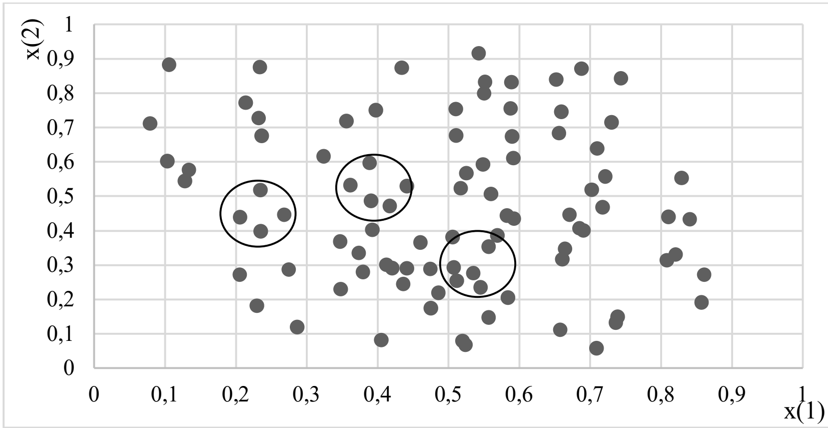

Figure 2. Schematic representation of cell creation in the phase space when calculating the approximated entropy

The specificity of the impulse complexity description provides reliable indicators that are resistant to the noise component, reflecting predetermined chaotic processes (phenomena) and random impulses using a combination of short sets, *N*, optimal thresholds, *r*, and lengths, *m* of the considered orders of counts.

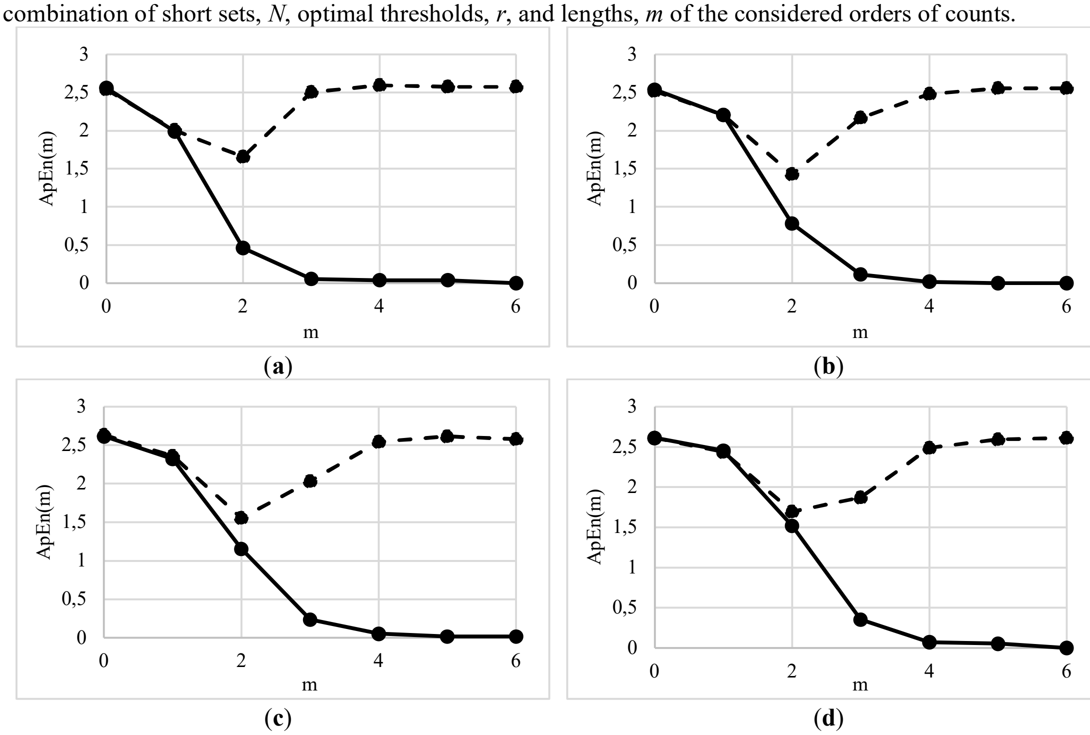

Figure 3. ApEn(m) and $ApEn_{cor}$(m) functions for the noise component with a set length N: a) 150, b) 300, c) 600, d) 1000 counts

Figures 1-3 illustrate the performance of the approximated entropy subsequent to signal processing according to the sequence delineated by formulas (3-7). Considering the above-mentioned factors, model experiments made it possible to evaluate the characteristics to identify the different components of each discrete process when the set length *N* was 150, 300, 600, and 1000 counts. Figure 3 shows several plots of the $ApEn(m)$ and $ApEn_{cor}(m)$ functions of the noise component for different set lengths. Analyzing the experimental results allows us to conclude that the reliability of each obtained chaotic characteristic of discrete impulse orders remains even when $N = 150$. The findings of the experiments demonstrated that stable entropy estimates were obtained for both extended and abbreviated sequences. Furthermore, we determined that fragments of signals with a length N equal to 300 samples were utilized.

Model experiments on the features of the approximated entropy showed that the impact of white noise on the system was efficiently eliminated if the value *r* characterizing this type of entropy was larger than the noise amplitude. An illustration of this fact is, for example, the results presented in Figure 4 obtained for a harmonic signal $s(i) = 3\,cos\left(\frac{\pi i}{20}\right)$, *i=1,…N*, containing noise *n*(*i*) uniformly distributed in the boundaries (-1, +1). Here, the considered sample *X*(*i*) appears as $X(i) = s(i) + cn(i)$, where *c* is an indicator that defines the amplitude of the noise component of the signal.

Thus, *ApEn*(*m*) values for all *m* except *m* = 1 are noise tolerant. When *c* < *r*, the value of *ApEn*(*m*=2,...,6) increases simultaneously with increasing *t* if the noise component becomes greater than the threshold *r*. In addition, *K*-entropy opens up the possibility of analyzing the noise of a predetermined impulse in the combined processes of $M_i(p)$. This is essential for analyzing biological impulses, because the predominant part of these impulses is composed of regular and random components.

The following relation expresses a mixed process:

$M_i(p) = [1 - Z_i(p)]X_i + Z_i(p)Y_i$, in this case, $X_i = \sqrt{2}\,sin\left(\frac{\pi i}{6}\right)$, *i=1,2,3,…; N* is a periodic impulse; Y_i is an independent random value in the limit of $(-\sqrt{3}; \sqrt{3})$; $Z_i(p)$ is a random value (if $Zi = 1$, the probability of this is expressed as *p*, and if $Z_i = 0$, the probability of this is (1-*p*)).

In other words, $M_i(p)$ is a combination of known and random components, where *p* represents the ratio of these components. The average value and magnitude of the typical deviation $M_i(p)$ correspond to zero and one, respectively; however, the current *p* does not determine them. Figure 5 shows the function *ApEn*(*m*=1,2,3,4,5) from the current *p* with respect to the considered model impulse. If the irregular component of the impulse corresponds to *ApEn*(*m*=1,2,3) and its intensity increases, the considered function will be nonlinear for significant values of p. For example, if *m* = 3, the value *ApEn*(*m*) decreases because the number of separate impulse orders increases simultaneously with the increase in *p*.

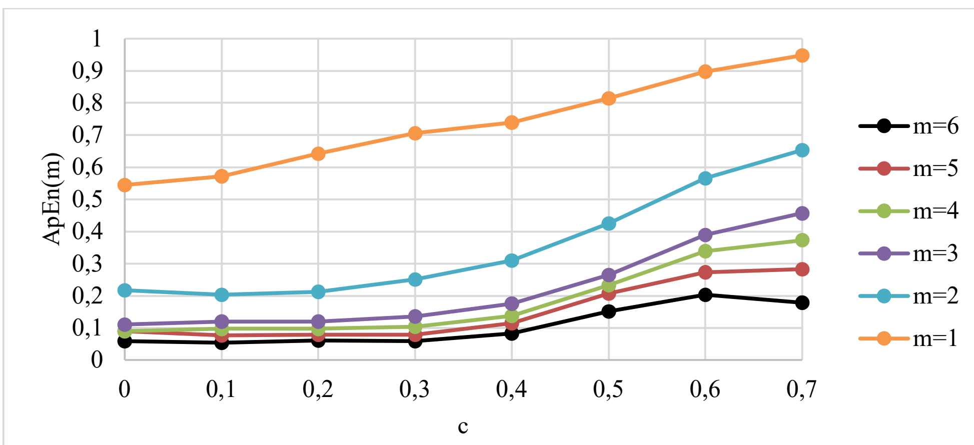

Figure 4. ApEN (m) function of the noise component

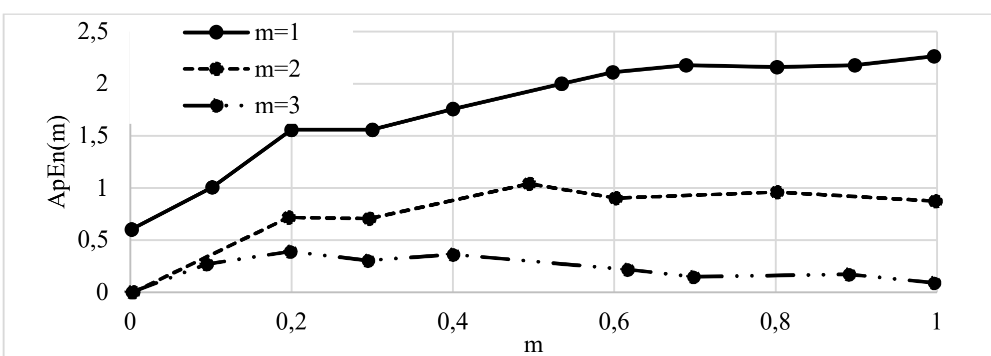

Figure 5. ApEN (m) function (m = 1, 2, 3, 4, 5) describing the change of random component in complex impulses

Some study results (essential for identifying signals with chaotic properties) are illustrated above, but others are not. For example, if the frequency of the harmonic impulse changes, it does not affect the current *ApEn*(m). Therefore, the approximate estimation of the K-entropy can help identify the dynamic irregularity established by a set of internal qualities of the process.

By analyzing the obtained dependencies *ApEn*(m) and $ApEn_{cor}(m)$ on m, we can conclude that the autoregressive process is a nondeterministic chaotic process. The nature of the dependencies *ApEn*(m) and $ApEn_{cor}(m)$ is similar to that of the regularities revealed in the case of white noise. A pronounced minimum $ApEn_{cor}(m)$ is observed; the values of *ApEn*(m) at small m are rather large, and with increasing m tends to zero, while the function $ApEn_{cor}(m)$ – tends to the value of absolute entropy.

In light of the analysis of the properties of the approximated entropy and the findings of the model experiments, it can be posited that the following parameters may be employed to gauge the extent of regularity observed in the changes occurring in a discrete sequence of samples:

– $ApEn_{cor}(m)$ and *ApEn*(m) values when m = 1, 2, 3, and 4 if the orders under consideration have negligible effects on the overall process.
– Conditional minima $ApEn_{cor}(m)$: $ME_K = ApEn(0) - \min\limits_{m=1\ldots6}\{ApEn(m)\}$ when m =1...6, which approximates the lower outlines of the K-entropy.

3.3. Construction of decision functions

The construction of decision functions from the approximated entropy estimates involves the use of linear discriminant analysis. In this analysis, the d-dimensional observations were projected onto a straight line. Rotating vector W in the original feature space allowed us to determine its orientation, such that the projected samples were well separated. This task is the goal of classical discriminant analysis. For AF detection, the detection of arrhythmias against the background of other rhythm disorders, discriminant analysis was performed for two groups: ω_1 (rhythmograms of atrial fibrillation) and ω_2 (normal rhythm). The obtained spectral density estimation can be used for the formation of spectral features and construction of appropriate solving rules. However, it is necessary to limit the analyzed frequency region, which reduces the dimensionality of the initial spectral representation and simplifies the implementation of the signal recognition procedures. For this purpose, we propose to estimate the discrepancy between the sampled frequency descriptions of signals by generating training data samples for the given classes ω_1 and ω_2 and calculating their spectral density estimates.

Fisher's criterion, which quantitatively assesses the quality of dividing observations into ω_1 and ω_2 classes, is defined by the following equation:

$$J = \frac{W^T * S_1 * W}{W^T * S_2 * W} \tag{8}$$

where S_1 is the between-class scatter matrix, S_2 is the within-class scatter matrix.

The linear separating function in the space of given features is defined by the following equation:

$$\text{If } D(X) > 0, then\ X \in \omega_1; \text{ if } D(X) < 0, then\ X \in \omega_2 \tag{9}$$

Vector W, which maximizes the value of criterion J, is in the form $W = S_2^{-1} * (m_1 - m_2)$, where m_1 and m_2 are vectors of the sample mean values for classes ω_1 and ω_2, respectively.

The value of the threshold w_0 was determined based on the criterion of optimality of partitioning into classes, specifically the minimization of the sum of errors of the first and second types. This approach was selected because it balances the importance of avoiding false negatives (missing the MA) with that of avoiding false positives (generating false alarms). To identify the errors, histograms of the distribution of projections of objects on the unit vector W for classes ω_1 and ω_2 were constructed, as well as the corresponding density functions of the distribution that adhere to the normal law of distribution.

Denoting the vector found above as W_1 the vector W_2 can be represented as follows: Let the matrix of coordinates of the objects in the original feature space be given as follows:

$$X = \begin{bmatrix} x_{1,1} & \cdots & x_{N,1} \\ \vdots & \ddots & \vdots \\ x_{1,d} & \cdots & x_{N,d} \end{bmatrix}$$

where d - is the number of features, N-number of objects.

We find vector W_1 by maximizing criterion J. Then, using the coordinate transformation $Y = X - W_1^T * X * W_1$ we determine the new coordinates of the objects:

$$Y = \begin{bmatrix} y_{1,1} & \cdots & y_{N,1} \\ \vdots & \ddots & \vdots \\ y_{1,d} & \cdots & y_{N,d} \end{bmatrix}$$

Similarly, we find the vector W_2 for the coordinates of objects $Y_i, i = 1, \dots, N$ in the residual space. After performing the appropriate transformations, the coordinates of vector W_2 were determined:

$$W_2^T = [0.357, -0.566, 0.744, -0.194]$$

Now, in the space (W_1, W_2), we find the best position of the new vector W' by rotating it within the angle -90°,...,+90 °relative to the direction of vector W_1. The average intergroup distance between the projections of objects of classes ω_1 and ω_2 to direction W' was calculated as follows:

Figure 6 shows the results of the distance calculation $\rho(\varphi)$ and the distribution of objects in space (W_1, W_2). The position of the new vector W' corresponds to the maximum value of $\rho(\varphi)$. Thus, the angle φ = 0,597 radians, and the coordinates of the vector W'^T = [0,827 0,562].

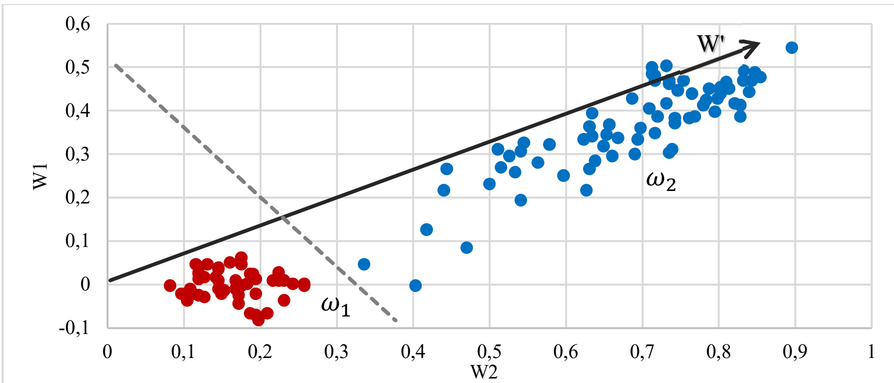

Figure 6. Visual representation of the separation of classes ω_1 and ω_2

3.4. Classification of atrial fibrillation

The basis for constructing decisive rules classifying AF types within the ω_1 class is the correlation rhythmogram of the CRG (scatterogram). It is a graphical representation on a plane in the form of points of each pair of neighboring RR intervals and reflects the degree of their linear dependence.

At present, scatterograms are constructed through the application of programmatic methodologies. In the construction of a scatterogram, a cluster of points is formed with the center located on the bisector of the right angle. The distance from the center of the cluster to the origin of the coordinate axes is proportional to the expected duration of the cardiac cycle. The value of the point deviation from the bisector indicates the degree to which the cardiac cycle in question is shorter or longer than the previous cycle. Deviations downward from the bisector indicated shorter cycles, whereas upward deviations indicated longer cycles. In the absence of any process variation or artifacts, the scatterogram point cloud typically assumes an ellipse-like form, situated symmetrically relative to the bisector, with the highest point density observed at the center of the group. A reduction in the size of the area under consideration indicated a decrease in the variability of cardiac cycles. In cases of arrhythmia, there is a notable dispersion of points, and the positioning of these accumulations enables the physician to visually ascertain the presence and nature of cardiac rhythm disturbance. In instances where statistical and spectral analyses of heart rate variability are inconclusive or inadequate, evaluation of scatterograms may offer a viable alternative. A training sample was constructed to study the characteristics of the distributions and develop solution rules. Five distinct types of rhythmograms and their corresponding scatterograms were identified to analyze atrial fibrillation (AF), and the corresponding solving rules were defined for each [28, 29]:

1. Monomodal symmetrical. Points are grouped in a relatively limited rounded area, and their pronounced thickening is located in the center, on the bisector at a right angle. In other words, there were a significant number of cardiac cycles with the same duration. This type is rare and only occurs in patients who do not receive foxglove preparations. This is based on the following rule.

$$Type\ 1 = (Z(f_{max}) \in b) \wedge \left(\sum_b f_b > \sum_{a,c} f_{a,c}\right) \wedge (f_{max} > 25)$$

2. The dataset is monomodal and asymmetric. A notable densification of points is observed on the bisector; however, their scattering area is constrained by straight lines parallel to the coordinate axes. The restriction of the point distribution area is indicative of the process of "filtering" of the most prevalent impulses in the atrioventricular junction. This is based on the following rule.

$Type\ 2 = (Z(f_{max}) \in A) \wedge (\sum_{Z\in A} f(Z) > \sum_{Z\in C} f(Z)) \wedge (f_{max} > 25)$

3. Amodal. The area of the point distribution is constrained by lines running parallel to the coordinate axes; however, there is no densification of the points on the bisector. This phenomenon is most frequently observed in patients receiving foxglove group drugs for an extended period. This is based on the following rule.
$Type\ 3 = (f_{max} \leq 25) \wedge (n_0 \leq 3) \wedge (\sigma(z) \leq 3{,}5)$

4. The distribution was polymodal. The points were distributed in a clustered manner along the angle bisector and parallel to the coordinate axes. The distance between the centers of the clusters of points is equal to 0.16–0.20 s (by type of atrial flutter), or less than 0.16 s (by type of large-wave fibrillation). This phenomenon has been observed in cases of atrial flutter with changing atrioventricular conduction and in patients with paroxysms of atrial fibrillation. This is based on the following rule.
$Type\ 4 = (f_{max} \leq 25) \wedge (n_0 > 3) \wedge (\sigma(z) > 3{,}5)$

5. The dataset is monomodal and inverted. The cluster of points is situated at the bisector in an area remote from the origin of coordinates, and is circumscribed by lines running parallel to the coordinate axes. This type is observed in patients who have ingested excessive amounts of foxglove-derived medications, resulting in documentation of numerous ventricular complexes at the atrioventricular junction. This is based on the following rule.
$Type\ 5 = (Z(f_{max}) \in C) \wedge (\sum_{Z\in C} f(Z) > \sum_{Z\in A} f(Z)) \wedge (f_{max} > 25)$

where $f_{max} = \max_Z f(Z)$; n_0 – is the number of symbols Z, for which $f(Z) = 0$; $\sigma(Z)$ – value of the standard deviation of the parameter Z; *a, b, A, B, C*- distribution areas $f(Z)$.

4. RESULTS

The experimental research presented here was based on data from the publicly available MIT-BIH Atrial Fibrillation Database, which can be accessed via PhysioNet. The database comprises 25 long-term ECG Holter records from diverse subjects that predominantly exhibit paroxysmal attacks. It encompasses two ECG signal channels with AF annotations. To investigate the frequency properties of the ECS, a sample of the verified signal fragments with a duration of 2 s was used. The addition of zeros to the obtained signal realizations enabled an interpolated estimate of the power spectral density (PSD) to be obtained, with a step equal to 0.244 Hz, with a sampling rate of 250 Hz, and the records also encompass manually marked beat notes by expert clinicians [30].

To analyze the performance of the proposed system, the generally accepted analysis methods are accuracy, specificity, and sensitivity.

Sensitivity = $\frac{TP}{TP+FN} * 100\%$, Specificity = $\frac{TN}{TN+FP} * 100\%$, Accuracy = $\frac{TN+T}{TN+TP+FN+F} * 100\%$

TP and TN indicate the numbers of correctly detected cases of atrial fibrillation and no atrial fibrillation, respectively. FP and FN indicate the number of incorrectly detected cases of atrial fibrillation and absence of atrial fibrillation, respectively.

The performance of the proposed methods is tested in two instances: definition of atrial fibrillation and classification of atrial fibrillation.

Table 1. Comparative analysis of AF diagnostic methods

Name of the method used	Sensitivity, %	Specificity, %	Accuracy, %	Reference
Multi-scale CNN	98,22	98,11	98,18	[31]
SVM + CNN	96.14	96.02	96.09	[32]
FNN	84,26	93,23	83,14	[33]
Threshold	99,2	97,3	98,1	[34]
LSTM + CNN	96,46	94,49	95,28	[35]
Proposed method, based on Kolmogorov approximation	98	98,5	98,4	

Most of the presented methods have been tested using the same MIT-BIH database. As evidenced by the results of the calculations presented in Table 1, the method demonstrated a high degree of sensitivity and specificity in the identification of atrial fibrillation, thereby rendering it suitable for application in practical tasks. Additionally, the method evaluated the impact of sample size on the precision of the analytical outcomes. The total error, comprising of primary and secondary errors (missed and false diagnoses, respectively), was selected as the evaluation criterion. The results of this analysis are shown in Figure 7.

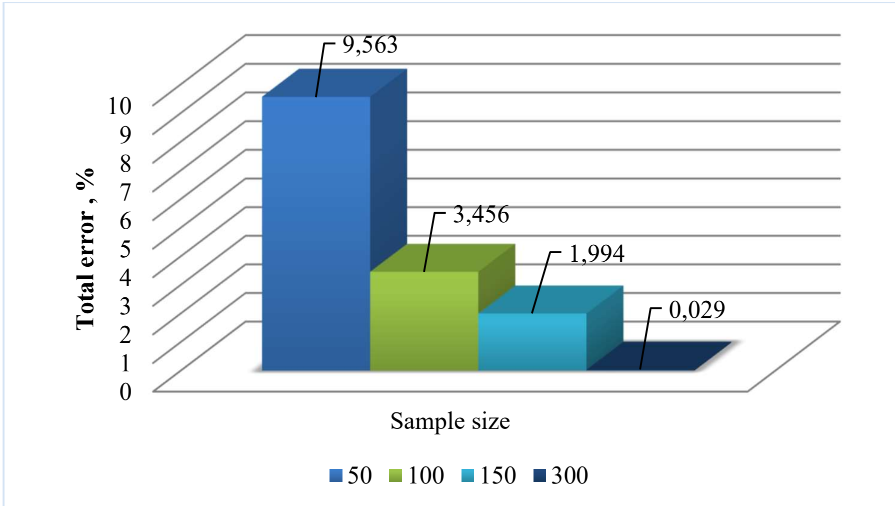

Figure 7. Results of the effect of sampling on the total error of the proposed method

The proposed method uses the parameters of approximate Kolmogorov entropy estimation, thus facilitating reliable detection of chaotic changes generated by nonlinear models. In addition to this capability, the method provided the smallest error rate of 2.5% in the identification of atrial fibrillation in the context of normal rhythms and frequent extrasystoles. In comparison with existing solutions for the recognition of atrial fibrillation, the proposed method demonstrated satisfactory results and facilitated substantial augmentation of the range of quantitative criteria for diagnosing cardiovascular system conditions. This augmentation is achieved through the utilization of a set of characteristics for deterministic chaos estimation. The incorporation of such systems in conjunction with a training method based on machine learning has the potential to enhance the capabilities and increase the accuracy of the presented method.

In the following section, the results of classifying the diagnosis of atrial fibrillation by type will be presented. As shown in Figure 8, the decisive rules had high sensitivity and specificity for all AF types. The lowest sensitivity (94%) was observed for the polymodal type (Type 4). Some signals of this type are categorized into amodal and monomodal asymmetric types. However, the polymodal type can be mixed with these types of arrhythmias, which affects the classification results. The diagnostic significance is not lost because the detection of amodal-type elements in the distribution indicates the inexpediency of electrical defibrillation of the heart.

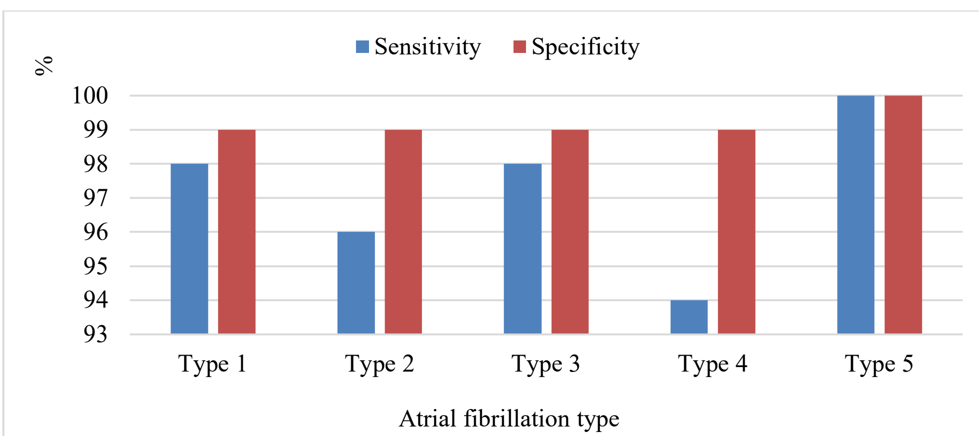

Figure 8. Efficacy of atrial fibrillation classification

The obtained results confirm the acceptable level of using the proposed method for solving practical problems. The results obtained in this study can be useful for the further development of methods and algorithms for polymodal data. The solution to such problems is most relevant and in demand in medical information systems and other areas of decision making in anthropotechnical systems [36-38].

5. CONCLUSIONS

Within the framework of this study, a linear discriminant analysis approach based on the concept of *K*-entropy was proposed to automate the procedure for recognizing AF against the background of other rhythm disorders using a limited data sample. The results of the experiments with model impulses confirmed that the methodology based on approximate *K*-entropy estimation allows for highly accurate detection of chaotic changes generated by a nonlinear model. We employed a linear discriminant analysis with the incorporation of conditional entropy parameters and approximate Kolmogorov entropy estimation to discern chaotic alterations in the sequence of cardiac cycles. This was performed with the objective of identifying atrial fibrillation amidst the backdrop of other rhythm disturbances. Identifying the type of AF is an essential indicator of the activity of any specialized professional because it is a highly informative diagnostic indicator that makes it possible to identify the features of atrioventricular nodal conduction, predict myocardial responses to defibrillation, and correctly select treatment courses based on cardiac drugs. The results of the proposed methods showed high accuracy, specificity, and sensitivity compared to existing topical methods. One of the limitations of the proposed method is the significant decrease in the accuracy of the results when dealing with low data sampling.

ACKNOWLEDGMENTS

Selected findings of this work were obtained under the grant agreement in the form of subsidies from the federal budget of the Russian Federation for state support for the establishment and development of world-class scientific centers performing R&D on scientific and technological development priorities dated April 20, 2022, No. 075-15-2022-307.

REFERENCES

[1] I. A. Alexandrov, A. V. Kirichek, V. Z. Kuklin, A. N. Muranov, and L. M. Chervyakov, "Developing the Concept of Methodological Support for Designing and Assessing the Efficiency of Information Protection Systems of Standard Information Systems Considering Their Vulnerabilities," *Journal of Computer Science*, vol. 19, no. 11, pp. 1305–1317, Oct. 2023.
[2] T. Pham, Z. J. Lau, S. H. A. Chen, and D. Makowski, "Heart Rate Variability in Psychology: A Review of HRV Indices and an Analysis Tutorial," *Sensors*, vol. 21, no. 12, p. 3998, Jun. 2021.
[3] I. A. Alexandrov, A. V. Kirichek, V. Z. Kuklin, and L. M. Chervyakov, "Development of an Algorithm for Multicriteria Optimization of Deep Learning Neural Networks," Hig*hTech and Innovation Journal*, vol. 4, no. 1, pp. 157–173, Mar. 2023.
[4] J. Son, J. Park, H. Oh, M. Bhuiyan, J. Hur, and K. Kang, "Privacy-Preserving Electrocardiogram Monitoring for Intelligent Arrhythmia Detection," *Sensors*, vol. 17, no. 6, p. 1360, Jun. 2017.
[5] V. Krasteva, I. Jekova, R. Leber, R. Schmid, and R. Abächerli, "Real-time arrhythmia detection with supplementary ECG quality and pulse wave monitoring for the reduction of false alarms in ICUs," *Physiological Measurement*, vol. 37, no. 8, pp. 1273–1297, Jul. 2016.
[6] E. Reganova, K. Solovyeva, D. Buyanov, A. Yu. Gerasimenko, and D. Repin, "Effects of Intermittent Hypoxia and Electrical Muscle Stimulation on Cognitive and Physiological Metrics." *Bioengineering,* vol. 10, no. 5, p. 536, Apr. 2023.
[7] S. R. SK, M. H. Kolekar, and R. J. Martis, "A Deep Learning Approach for Detecting Atrial Fibrillation using RR Intervals of ECG," *Frontiers in Biomedical Technologies,* Apr. 2024.
[8] R. Czabanski et al., "Detection of Atrial Fibrillation Episodes in Long-Term Heart Rhythm Signals Using a Support Vector Machine," *Sensors*, vol. 20, no. 3, p. 765, Jan. 2020.
[9] D. M. Harmon, O. Sehrawat, M. Maanja, J. Wight, and P. A. Noseworthy, "Artificial Intelligence for the Detection and Treatment of Atrial Fibrillation," *Arrhythmia & Electrophysiology Review*, vol. 12, Apr. 2023.
[10] R. A. Borracci, J. D. M. Pulvet, C. A. Ingino, M. Fitz Maurice, A. H. Prado, and E. Dominé, "Geometric patterns of time-delay plots from different cardiac rhythms and arrhythmias using short-term EKG signals," *Clinical Physiology and Functional Imaging*, vol. 38, no. 5, pp. 856–863, Dec. 2017.
[11] N. R, S. K. Bv, A. Rawat, and S. S, "Cardiac Arrhythmia - Prediction and Classification using Support Vector Machine," *2021 International Conference on System, Computation, Automation and Networking (ICSCAN)*, pp. 1–4, Nov. 2023.
[12] N. Nuryani, B. Harjito, I. Yahya, and A. Lestari, "Atrial fibrillation detection using support vector machine," *Proceedings of the Joint International Conference on Electric Vehicular Technology and Industrial, Mechanical, Electrical and Chemical Engineering,* vol. 93, pp. 215–218, Nov. 2015.
[13] A. Kumar, H. Tomar, V. K. Mehla, R. Komaragiri, and M. Kumar, "Stationary wavelet transform based ECG signal denoising method," *ISA Transactions*, vol. 114, pp. 251–262, Dec. 2020.
[14] M. Arumugam and A. K. Sangaiah, "Arrhythmia identification and classification using wavelet centered methodology in ECG signals," *Concurrency and Computation Practice and Experience*, vol. 32, no. 17, Nov. 2019.

[15] X. Chen et al., “Atrial fibrillation detection based on multi-feature extraction and convolutional neural network for processing ECG signals,” *Computer Methods and Programs in Biomedicine*, vol. 202, p. 106009, Feb. 2021.
[16] H. Ashikaga et al., “Quantitative Assessment of Atrial Regional Function Using Motion Estimation Computed Tomography,” *Journal of Computer Assisted Tomography*, vol. 38, no. 5, pp. 773–778, Jan. 2014.
[17] P. Lyakhov, M. Kiladze, and U. Lyakhova, “System for Neural Network Determination of Atrial Fibrillation on ECG Signals with Wavelet-Based Preprocessing,” *Applied Sciences*, vol. 11, no. 16, p. 7213, Aug. 2021.
[18] A. F. Gündüz and M. F. Talu, “Atrial fibrillation classification and detection from ECG recordings,” *Biomedical Signal Processing and Control*, vol. 82, p. 104531, Dec. 2022.
[19] S. A. Lubitz, A. Z. Faranesh, C. Selvaggi, S. J. Atlas, D. D. McManus, D. E. Singer, S. Pagoto, M. V. McConnell, A. Pantelopoulos, and A. S. Foulkes, “Detection of Atrial Fibrillation in a Large Population Using Wearable Devices: The Fitbit Heart Study.” *Circulation,* vol. 146, no. 19, pp. 1415–1424, Oct. 2022.
[20] F. Murat, F. Sadak, O. Yildirim, M. Talo, E. Murat, M. Karabatak, Y. Demir, R. Tan, and U. Rajendra Acharya, “Review of Deep Learning-Based Atrial Fibrillation Detection Studies.” *International Journal of Environmental Research and Public Health,* vol. 18, no. 21, p. 11302, Oct. 2021.
[21] K. Aihara and H. Suzuki, “Theory of hybrid dynamical systems and its applications to biological and medical systems,” *Philosophical Transactions of the Royal Society a Mathematical Physical and Engineering Sciences*, vol. 368, no. 1930, pp. 4893–4914, Oct. 2010.
[22] L. Tang, H. Lv, F. Yang, and L. Yu, “Complexity testing techniques for time series data: A comprehensive literature review,” *Chaos Solitons & Fractals*, vol. 81, pp. 117–135, Sep. 2015.
[23] J. A. Gómez-García, J. I. Godino-Llorente, and G. Castellanos-Dominguez, “Non uniform Embedding based on Relevance Analysis with reduced computational complexity: Application to the detection of pathologies from biosignal recordings,” *Neurocomputing*, vol. 132, pp. 148–158, Oct. 2013.
[24] M. D. Todd, J. M. Nichols, L. M. Pecora, and L. N. Virgin, “Vibration-based damage assessment utilizing state space geometry changes: local attractor variance ratio,” *Smart Materials and Structures*, vol. 10, no. 5, pp. 1000–1008, Oct. 2001.
[25] A. A. Tatarkanov, I. A. Alexandrov, L. M. Chervjakov, and T. V. Karlova, “A Fuzzy Approach to the Synthesis of Cognitive Maps for Modeling Decision Making in Complex Systems,” Emerging Science Journal, vol. 6, no. 2, pp. 368–381, Mar. 2022.
[26] A. H. Lampezhev, E. Y. Linskaya, A. A. Tatarkanov, and I. A. Alexandrov, “Cluster Data Analysis with a Fuzzy Equivalence Relation to Substantiate a Medical Diagnosis,” *Emerging Science Journal*, vol. 5, no. 5, pp. 688–699, Oct. 2021.
[27] A. Tatarkanov, I. Alexandrov, A. Muranov, and A. Lampezhev, “Development of a Technique for the Spectral Description of Curves of Complex Shape for Problems of Object Classification,” *Emerging Science Journal*, vol. 6, no. 6, pp. 1455–1475, Dec. 2022.
[28] H. Zhang, C. Liu, F. Tang, M. Li, D. Zhang, L. Xia, S. Crozier, et al., “Atrial Fibrillation Classification Based on the 2D Representation of Minimal Subset ECG and a Non-deep Neural Network.” *Frontiers in Physiology,* vol. 14, Feb. 2023.
[29] P. Yu. Timofeeva, B. E. Alekseev, L. A. Manilo, and A. P. Nemirko, “An Algorithm for Automated Representation of Dynamic Correlation Rhythmograms for Long-lasting Signal Recordings.” *Biomedical Engineering,* vol. 54, no. 5, pp. 357–360, Jan. 2021.
[30] A. L. Goldberger et al., “PhysioBank, PhysioToolkit, and PhysioNet,” *Circulation*, vol. 101, no. 23, Jun. 2000.
[31] X.-C. Cao, B. Yao, and B.-Q. Chen, “Atrial Fibrillation Detection Using an Improved Multi-Scale Decomposition Enhanced Residual Convolutional Neural Network,” *IEEE Access*, vol. 7, pp. 89152–89161, Jan. 2019.
[32] C. Ma, S. Wei, T. Chen, J. Zhong, Z. Liu, and C. Liu, “Integration of Results From Convolutional Neural Network in a Support Vector Machine for the Detection of Atrial Fibrillation,” *IEEE Transactions on Instrumentation and Measurement*, vol. 70, pp. 1–10, Dec. 2020.
[33] Y. Chen, C. Zhang, C. Liu, Y. Wang, and X. Wan, “Atrial Fibrillation Detection Using a Feedforward Neural Network,” *Journal of Medical and Biological Engineering*, vol. 42, no. 1, pp. 63–73, Feb. 2022.
[34] I. A. Marsili et al., “Implementation and validation of real-time algorithms for atrial fibrillation detection on a wearable ECG device,” *Computers in Biology and Medicine*, vol. 116, p. 103540, Nov. 2019.
[35] X. Zhang, J. Li, Z. Cai, L. Zhang, Z. Chen, and C. Liu, “Over-fitting suppression training strategies for deep learning-based atrial fibrillation detection,” Medical & Biological Engineering & Computing, vol. 59, no. 1, pp. 165–173, Jan. 2021.
[36] V. A. Gorelov, E. Yu. Linskaya, A. A. Tatarkanov, I. A. Alexandrov, and S. A. Sheptunov, “Complex Methodological Approach to Introduction of Modern Telemedicine Technologies into the Healthcare System on Federal, Regional and Municipal Levels,” *2020 International Conference Quality Management, Transport and Information Security, Information Technologies*, vol. 14, pp. 468–473, Sep. 2020.
[37] D. V. Polezhaev, A. A. Tatarkanov, and I. A. Alexandrov, “Forming the Architecture of a Multi-Layered Model of Physical Data Storage for Complex Telemedicine Systems,” *HighTech and Innovation Journal*, vol. 4, no. 4, pp. 797–810, Dec. 2023.
[38] I. A. Alexandrov, V. Z. Kuklin, A. N. Muranov, and A. A. Tatarkanov, “Theoretical Foundations of an Algorithm of Visualization of a Set of Points of a Multidimensional Space for Use in Anthropotechnical Decision Support Systems,” *Proceedings of the Institute for System Programming of RAS*, vol. 34, no. 4, pp. 201–210, Jan. 2022.

BIOGRAPHY OF AUTHORS

Abas Lampezhev was born in Severomorsk, Russia. He received a MSc in Bauman Moscow State Technical University in the field of navigation and ballistic support for the use of space technology in 2020. He is a researcher in a field of system analysis, decision-making methods, multi-parameter optimization and mathematical modeling. He works as a researcher at the Institute of Design and Technology Informatics of the Russian Academy of Sciences. He has some important published papers in international journals.

Naur Ivanov was born in Nalchik, Russia. He received a MSc in Rocket and space composite structures at N.E. Bauman Moscow State Technical University in 2017. He obtained his postgraduate degree at the A.A. Blagonravov Institute of Mechanical Engineering of the Russian Academy of Sciences in 2021. He works as a researcher at the Institute of Design and Technology Informatics of the Russian Academy of Sciences. He has some important published papers in international journals.

Tagirbek Aslanov was born in Makhachkala, Russia. He received a MSc in Autonomous information and control systems at N.E. Bauman Moscow State Technical University in 2011. He holds a technical PhD in Bauman Moscow State Technical University that he received in 2015. He became an Associate Professor at Dagestan State Technical University in 2015. He works as a senior researcher at the Institute of Design and Technology Informatics of the Russian Academy of Sciences. He has some important published papers in international journals.

Muhamed Nogmov was born in Nalchik, Russia. Received a MSc in Robotics systems and mechatronics at N.E. Bauman Moscow State Technical University in 2014. Now he is a postgraduate student at the Institute of Design and Technology Informatics of the Russian Academy of Sciences. He works as a researcher at the Institute of Design and Technology Informatics of the Russian Academy of Sciences. He has some important published papers in international journals.

Viktor Lysenko was born in Nalchik, Russia. He received a MSc in Spacecraft and carrier rockets at N.E. Bauman Moscow State Technical University in 2016. Now he is a postgraduate student at the Institute of Design and Technology Informatics of the Russian Academy of Sciences. He works as a junior researcher at the Institute of Design and Technology Informatics of the Russian Academy of Sciences. He has some important published papers in international journals.